# MAGNETIC PROPERTIES OF UNDULATOR VACUUM CHAMBER MATERIALS FOR THE LINAC COHERENT LIGHT SOURCE*

Soon-Hong Lee[#], Isaac Vasserman, Shigemi Sasaki, Dean Walters,
Advanced Photon Source, ANL IL 60439, USA
Dong-Eon Kim , Pohang Accelerator Laboratory, Pohang, KOREA

*Abstract*

A prototype vacuum chamber is being developed at the Advanced Photon Source (APS) for use in the Linac Coherent Light Source at Stanford Linear Accelerator Center. The chamber will be fabricated from austenite stainless steel that is generally regarded as nonmagnetic in the annealed condition and not attracted significantly by a magnet. However, cold working or welding will change its magnetic properties. This paper presents measurements used to choose a proper vacuum chamber material for the LCLS undulator by examining the fabrication processes and investigating the relative magnetic permeability of the austenite stainless steels. In addition, the magnetic field variations under APS undulator A with/without 3-inch-long vacuum chambers and numerical studies of nonunity magnetic permeable vacuum chambers are presented.

## INTRODUCTION

The Linac Coherent Light Source (LCLS) is a high-brightness x-ray free-electron laser (FEL) project that will be constructed at Stanford Linear Accelerator Center (SLAC). The primary goal of the LCLS is the production and saturation of FEL radiation over the 1.5~15 Å wavelength range from a high-energy electron beam accelerated through 1/3 of the 2 mile SLAC linac. The radiation wavelength will be controlled through the electron beam energy over the 4.31~13.64 GeV range, and a total number of $10^{12}$ FEL photons per pulse will be produced at the short end of the LCLS wavelength range. To do that, the electron beam will pass through an array of 33 separate undulator segments to produce spontaneous and FEL x-ray radiation. The total length of the undulator will be 131.52 m long, which includes 3.4-m-long undulator segment strongbacks, 0.470 m short breaks, and 0.898 m long breaks. Currently, a prototype vacuum chamber for LCLS undulator segments is under development at the Advanced Photon Source (APS) [1].

One of the important considerations in design of the vacuum chamber is the impedance that the vacuum chamber presents to the beam. There are three main contributors to the impedance of the vacuum chamber, i.e., its electrical surface conductivity, its surface roughness, and its geometric shape. The goal is to keep the contribution from surface roughness and geometric shape small (less then 10 %) compared to the contribution from the finite electrical conductivity. The surface roughness impedance is dependent on the longitudinal spatial spectrum of the surface roughness. For each spatial frequency component of the surface roughness, the ratio of the corresponding spatial wavelength to the amplitude will be greater or equal to 300 over the 0.01-10 mm period range.

The initial chamber design was a round shaped copper tube. But, the physics calculations showed that the round copper tube would result in an unacceptably large energy variation induced within the bunch over the length of the undulator (~0.6%) due to the AC resistive wall wakefield [2]. However, if we use a flat aluminum chamber, the energy variation can be reduced to within acceptable limits (<0.2%). Due to smaller AC conductivity wakefields for aluminum than copper, a chamber development program was newly organized to measure the AC conductivity in the range of wavelengths from 10 to 100 microns. Measurements with pure copper (C10100) and pure aluminum (99.99%) samples were performed at Brookhaven National Laboratory [3]. The results were compared with theory and showed that aluminum is a better selection than copper.

Based on the experiments and the theoretical study, stainless steel with a rectangular shape and a coated layer of minimum thickness 100 nm aluminum was considered as a vacuum chamber material. The width of the chamber will be more than 50 % larger than its height; so, the inner dimensions of the vacuum chamber inside the undulator segment will be 5 mm in height and 10 mm in width. The design utilizes a polished flat stainless steel sheet that is folded and welded to the stainless steel strong-back holding arm. Hence, the question arises as to how mechanical cold working of the stainless steel and the associated change in magnetic properties will influence the magnetic field in the undulator segments. In general, the magnetic properties of austenite stainless steels are affected by their compositions, processing methods and physical conditions, though the stainless steels are considered nonmagnetic in the annealed condition and not attracted significantly by a magnet. However, cold working or welding may significantly change their magnetic properties. The change occurs because the cold work and welding deformation induces a transformation of the microstructure from austenite to martensite.

This study will facilitate choice of a proper material for the LCLS undulator vacuum chamber by examining the fabrication processes and investigating the relative magnetic permeability of candidate materials, which have been chosen from published studies [4, 5]. In addition, the magnetic field variations under APS undulator A (a hybrid permanent magnet undulator with a 33 mm period) with/without 3-inch-long chambers fabricated from

* Work supported by DOE under contract no. W-31-109-Eng-38.
# slee@aps.anl.gov

sample materials and the numerical studies of nonunity magnetic permeable vacuum chambers are presented.

## TEST & SIMULATION DESCRIPTIONS

### *Samples*

The materials considered for use in the LCLS vacuum chamber are austenite stainless steels, such as 316LN, 20Cb-3, Nitronic 33, Nitronic 40, and 310S. The 316LN (UNS S 31653) is Ni-strengthened stainless steel and is stronger than 316L without adversely affecting nonmagnetic properties. It is well known as a low magnetic permeable material. However, the plate and sheet/strip type for use in the LCLS application is not commercially available, and rebar has been the primary application in the U.S. Some are available in Europe and Asia, but, the manufacturer keeps production down. The 310/310S (UNS S 31000) is austenitic Cr-Ni stainless steel and has excellent resistance to oxidizing and carburizing atmospheres, which can be used in applications involving sulfur-bearing gases at elevated temperature. Nitronic 33® (UNS S24000, XM-29®) is Mg- and Ni-strengthened austenitic Cr-Ni stainless steel. Magnetic permeability remains low after severe cold working at cryogenic temperatures. Nitronic 33® is stronger than conventional stainless steels, but the same fabricating equipment and techniques can generally be used. Nitronic 40® (UNS S21900, XM-10®) has high-temperature oxidation resistance and excellent toughness at cryogenic temperatures. Applications include aircraft components, chemical and pollution-control equipment. The 20Cb-3® (UNS N08020, Alloy 20) has excellent mechanical properties and comparative ease of fabrication. This material is known to have very low permeability when annealed and even cold work.

The 316LN plate of 1" x 20" x 25" was provided from PAL, Korea. Other samples, ordered from Metal Sample Company, are 1/16" and 1/4" thick 3" x 3" plates and strips. But, only 5/16" thick material was available for Nitronic 33, so it was cut using wire-EDM to be 1/16" and 1/4" thick. In the case of Nitronic 40, only 3/16" thick material was available, so the chamber for Nitronic 40 was relatively thinner than the other chambers.

### *Tests and Fabrication of Chambers*

Permeability is the property used to measure how well a material concentrates the magnetic field. It gives an indication of the strength of the attraction to a magnet. The permeability of samples under the following conditions: as-received, after annealing, after cold working (cutting, forming, milling), after welding, and after machining, etc., was measured using a Ferromaster permeability meter (Stefan Mayer Instruments, Germany). Its sensitivity is a function of the sample thickness. The data were converted from the measured permeability values based on the sensitivity, which is defined as $(\mu_{measured}-1)/(\mu_{true}-1)$.

The as-received samples were annealed at 1,750ºF for 30 minute for the 20Cb-3 sample and 1,950ºF for 30 minutes for all other types at a vacuum level less than 1.0 x $10^{-4}$ Torr. For rapid quenching, nitrogen gas was used to cool down the samples and vacuum oven.

Figure 1: Test setups for measurement of magnetic permeability using a Ferromaster (left) and variation of applied magnetic fields using undulator A (right).

To examine the influence of cold working on the magnetic permeability, a short length of vacuum chamber that covered two magnetic periods was fabricated. At each fabrication step, magnetic permeability was remeasured to see if any variation occurred. In addition, to investigate high magnetic field influence to relative magnetic permeability, a 3-inch-long vacuum chamber was inserted into APS undulator A with an 8 mm gap and a field of ~1.2 Tesla was applied, as shown in Fig. 1. Then, variations of the applied magnetic fields without the sample chamber were compared.

Furthermore, Lakeshore's 7400 series vibrating sample magnetometer (VSM) was used to measure the magnetic properties of the annealed sample specimen (1 mm x 1 mm x 7 mm) without cold working.

### *Numerical Simulations*

The effect of the nonunity permeability of stainless steel vacuum chambers was simulated using the ANSYS finite element (FE) code, and the error field was estimated based on the following definition;

$$\Delta B(z) = B(z, \mu = nonlinear) - B(z, \mu = 1)\,. \qquad (1)$$

The data in Fig. 2 were used to describe the nonlinear magnetic properties of the materials.

In the FE model, the inner flat aperture of the vacuum chamber was set to 10 mm (W) x 5 mm (V) with 5 mm diameter on one of the side walls, as shown in Fig. 3. The following simulations were performed;

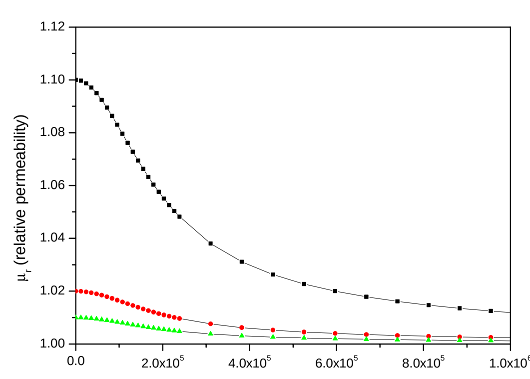


Figure 2: Nonlinear permeability used in the analysis.

- A 0.5 mm thin-walled chamber with peak permeability of 1.100.
- A 0.5 mm thin-walled chamber with 10 mm long holding arm and peak permeability of 1.100.
- 0.5 mm thin-walled chamber with 10 mm long holding arm and 3 different peak permeability of 1.020 in a bended area, 1.100 in the welded area of 1 mm x 1 mm, and 1.010 in other area.

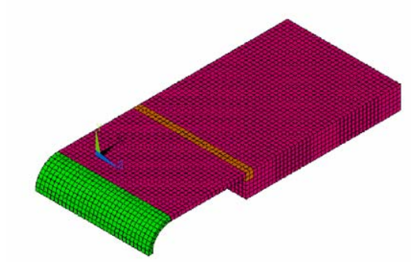

Figure 3: ANSYS FE simulation model for the vacuum chamber.

## RESULTS AND DISCUSSION

Table 1 summarizes the permeability measurement results under the fabrication processes of the vacuum chamber and represents the permeability in terms of the sample thickness. Data in parenthesis refer to the true permeability of the holding arm, which were converted from the measured thickness of 4.76, 6.0, 6.35, 6.65 mm. Others refer to the true permeability of the thin-walled area, which were converted from the measured thickness of 0.5, 1.59, 1.99 mm. Samples received from the vendor had low permeability values of less than 1.010. But, the preparation of samples was not known, so all samples were annealed. After annealing, the permeability was measured again. The results showed Nitronic 33 and 20Cb-3 had increased in permeability and confirmed the previous measurement results [3]. Then, the annealed 1/16" samples were formed into U-shaped channels and the 1/4" samples were machined / ground prior to welding. The permeability of each sample was checked again after forming and machining. Permeability changes after forming and machining were not significant. Nitronic 33 samples showed the most changes.

The formed and the ground samples were then TIG-welded together to build 3-inch-long vacuum chambers as shown in Fig. 4. Permeability was measured at a minimum of 4 places along the welded centerline on each side. The permeability of 310S and the Nitronic series had increased after TIG welding, with no changes in 316LN. Although 20Cb-3 had a small increase in permeability, it had a very narrow heat-affected zone (HAZ), and good weldability. Furthermore, vacuum chamber weldments were then machined to have holes with a 6 mm vertical dimension as shown in Fig. 5.

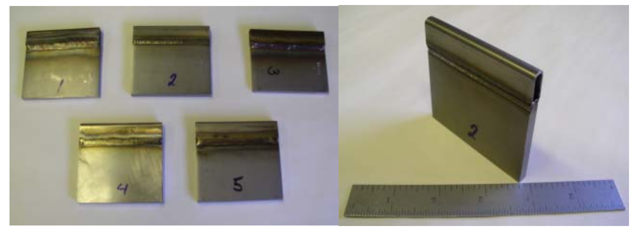

Figure 4: After welding (left 1: Nitronic 33, 2: 20Cb-3, 3: Nitronic 40, 4: 316LN, 5: 310S; right 20Cb-3)

Figure 5: After machining (left 1: 316LN, 2: 20Cb-3, 3: Nitronic 33, 4: Nitronic 40, 5: 310S; right 20Cb-3)

The permeability in the holding arm area had decreased, except in Nitronic 40. But, in the thin-walled area on the top and bottom, all samples had increased in permeability except Nitronic 40. Because the Ferromaster permeability meter is very sensitive to sample thickness, especially when less than 2 mm, the last two columns in Table 1 represent results very difficult to analyze. The calculation from measured to true permeability is possibly biasing the results as a result of using the final dimensions after the last machining step.

Throughout the fabrication studies, we confirmed that 316LN is the only material without any practical changes in permeability and that 20Cb-3 has low permeability and good weldability.

Table 1: Magnetic permeability measurements using Ferromaster under the various fabrication conditions.

| Material | As-received condition | After vacuum annealing | After machining & forming | After TIG welding | After final machining |
|---|---|---|---|---|---|
| 316LN | 1.002$^{a}$ (1.004$^{b}$) | 1.003$^{a}$ (1.003$^{b}$) | 1.003$^{a}$ (1.003$^{b}$) | 1.004$^{a}$ (1.003$^{b}$) | 1.008$^{c}$ (1.003$^{d}$) |
| 310S | 1.057$^{e}$ (1.005$^{f}$) | 1.036$^{e}$ (1.003$^{f}$) | 1.033$^{e}$ (1.003$^{f}$) | 1.042$^{e}$ (1.018$^{f}$) | 1.051$^{c}$ (1.007$^{d}$) |
| 20Cb-3 | 1.007$^{e}$ (1.008$^{f}$) | 1.008$^{e}$ (1.015$^{f}$) | 1.008$^{e}$ (1.015$^{f}$) | 1.010$^{e}$ (1.011$^{f}$) | 1.018$^{c}$ (1.009$^{d}$) |
| Nitronic 33 | (1.002$^{g}$) | 1.022$^{e}$ (1.006$^{f}$) | 1.030$^{e}$ (1.012$^{f}$) | 1.030$^{e}$ (1.023$^{f}$) | 1.126$^{c}$ (1.033$^{d}$) |
| Nitronic 40 | 1.004$^{e}$ (1.003$^{h}$) | 1.003$^{e}$ (1.004$^{h}$) | 1.005$^{e}$ (1.004$^{h}$) | 1.019$^{e}$ (1.052$^{h}$) | 1.081$^{c}$ (1.048$^{h}$) |
| Calibration, 1.27±.01 | 1.272 | 1.276 | 1.275 | 1.277 | 1.276 |

Sample thickness when measured $^{a}$: 1.99 mm, $^{b}$: 6.65 mm, $^{c}$: 0.5 mm, $^{d}$: 6.0 mm, $^{e}$: 1.59 mm, $^{f}$: 6.35 mm, $^{g}$: 7.94 mm, $^{h}$: 4.76 mm

The permeability of the annealed samples without any cold work was measured by using VSM, as shown in Fig. 6. We found that all the samples have a very low permeability of less than 1.010 and are saturated in magnetic fields of 6,000 Gauss. Nitronic 33, Nitronic 40 and especially 316LN all have very low permeability (less than 1.005) when the material has not been cold worked. However, based on the Ferromaster measurements, the Nitronic series and 310S showed high permeability and are sensitive to welding and machining.

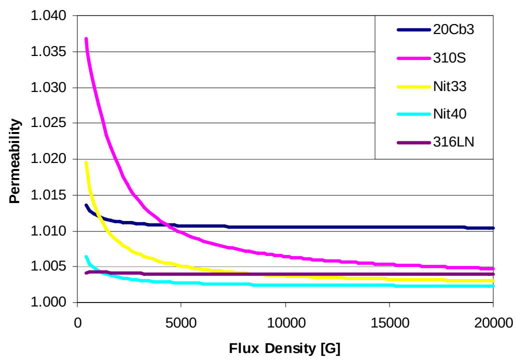


Figure 6: Magnetic permeability (without cold work) measured with Lakeshore's 7400 series vibrating sample magnetometer.

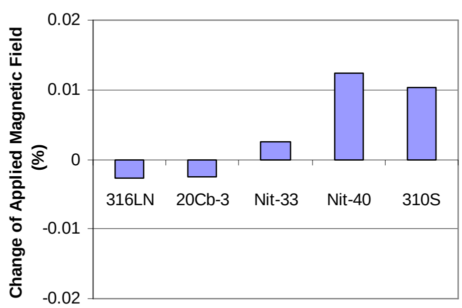


Figure 7: Relative change of applied magnetic fields.

Under APS undulator A, we measured the relative changes in applied magnetic fields at peak point with/without 3-inch-long vacuum chambers, as shown in Fig. 7. In this application, we applied a peak magnetic field of 1.2 Tesla and the acceptable range of the change of applied magnetic field is $\Delta B/B < 1.5 \times 10^{-4}$. Based on the results of the changes to the applied magnetic field, all vacuum chamber materials can be considered suitable for the LCLS vacuum chambers.

Finally, Fig. 8 shows the changes of magnetic fields from the FE simulations in the half period along the beam direction, to see the effect of the nonunity permeability of stainless steel vacuum chambers. Without the holding arm (black dot), 2.5 Gauss changes were obtained at the maximum field. With a holding arm (red dot), which dominates the volume, the shielding effect might be dominated by the holding arm. So, the maximum field change obtained was smaller than 4 Gauss, and the sign of field was changed. For both cases, we assumed that the whole chamber had the peak permeability of 1.100. However, if 3 different permeability values in the structure are assumed (green dot), the maximum field change obtained was close to 1 Gauss. This would be the result from volume reduction of the high permeable part. In addition, this result looks consistent with the permeability measurements for 20Cb-3 using the Ferromaster and APS undulator A.

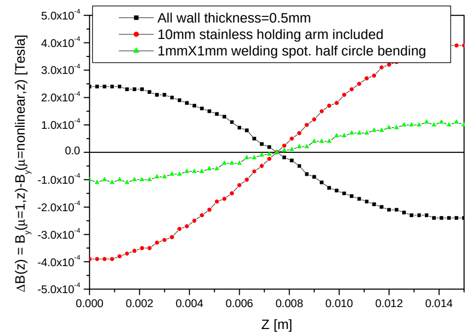


Figure 8: Absolute change of magnetic fields from the FE simulations in the half period along the beam direction.

## CONCLUSION

Based on the magnetic measurements of sample materials, 316LN stainless steel underwent no significant changes in magnetic permeability throughout the fabrication processes. Without cold working, 316LN, Nitronic 33, and Nitronic 40 had very low permeability (less than 1.005). But Nitronic 33, Nitronic 40, and 310S were very sensitive to the welding process, which increased the permeability values to over 1.020. Results of the APS undulator A measurements and FE simulations showed that the changes of magnetic field applied to the chambers were within the acceptable range of less than 2 Gauss. Thus, stainless steel 316LN is recommended for use where low magnetic permeability is required, such as LCLS vacuum chambers. In addition, as alternative materials for LCLS vacuum chambers, materials that retain low permeability after welding, like 20Cb-3 and cost-effective material like 310S, can be considered.

## ACKNOWLEDGMENTS

The authors would like to thank Drs. J. Samuel Jiang and Y. Choi at the Material Science Division, Argonne for VSM sample measurements.

## REFERENCES

[1] LCLS Physics Requirements Document # 1.4–001.
[2] K. Bane and G. Stupakov, "Resistive wall wakefield in the LCLS undulator beam pipe," LCLS-TN-04-11.
[3] Private communication, J.J. Tu.
[4] N. Wilson and P. Bunch, "Magnetic Permeability of Stainless Steel for Use in Accelerator Beam Transport Systems," PAC1991 – 2322.
[5] S. Yadav, "Magnetic Permeability of Stainless Steels at Low Temperature," TD-01-065, Fermi National Accelerator Laboratory, September 27, 2001.